The Journal of Experimental Biology 210, 3209-3217
Published by The Company of Biologists 2007
doi:10.1242/jeb.008367

An isolated insect leg's passive recovery from dorso-ventral perturbations

Daniel M. Dudek* and Robert J. Full

Department of Integrative Biology, University of California at Berkeley, Berkeley, CA 94720-3140, USA

*Author for correspondence at present address: Department of Zoology, University of British Columbia, Vancouver, BC V6T 1Z4, Canada (e-mail: dudek@zoology.ubc.ca)

Accepted 2 July 2007

Summary

Cockroaches recover rapidly from perturbations during high-speed running that allows them to cross unstructured terrains with no change in gait. Characterization of the exoskeletal material properties of the legs suggests that passive mechanical feedback could contribute to the self-stabilizing behavior. We imposed large, dorsal-ventrally directed impulsive perturbations to isolated hind legs having both a fixed and free body–coxa joint and measured their recovery. We tested a frequency-independent hysteretic damping model that effectively predicted the behavior of sinusoidal oscillations of isolated legs. Leg position reached its peak amplitude within 4–6 ms following an impulse. Position was 99% recovered within 16±3.3 ms for the stiffest possible leg configuration and within 46±6.6 ms for the most compliant leg configuration. The rapid recovery supports the hypothesis that passive musculo-skeletal properties play an important role in simplifying the control of high-speed locomotion.

Key words: locomotion, biomechanics, modeling, *Blaberus discoidalis.*

Introduction

Animals are capable of stably running across highly unstructured terrains, where surface compliance varies greatly, reliable footholds can be infrequent, and legs are likely to be perturbed. Maintaining stability under such conditions is a complex task involving the interaction between the passive material properties of the skeletal system and tissues, the intrinsic properties of muscle [including preflexes (Brown and Loeb, 2000)], and the nervous system (Cruse, 1990; Wilson, 1966), which must accommodate, and potentially modify, the musculo-skeletal mechanics. Since perturbations to the leg trajectories are the norm rather than the exception, we hypothesize that passive dynamic self-stabilization can simplify the control of rapidly traversing uneven surfaces. By passive self-stabilization we refer to recovery back to a limit cycle in the absence of neural feedback from reflexes. By dynamic we refer to systems in which motion and kinetic energy must be considered.

Passive self-stabilization has been identified as an important factor in recovering from unexpected perturbations, and can arise from both the material properties of the joints and skeleton as well as from the dynamics of the center of mass (COM) (Holmes et al., 2006). The dynamics of the COM of an array of morphologically diverse terrestrial runners can be modeled as self-stabilizing spring-mass systems in both the sagittal and horizontal planes (Ghigliazza et al., 2005). Humans rapidly alter leg stiffness prior to neural reflex action to maintain similar COM trajectories when substrate compliance changes unexpectedly (Moritz and Farley, 2004), and guinea fowl maintain dynamic stability when encountering an unexpected change in substrate height due in part to changed muscle moment arms and preflexes (Daley et al., 2007; Daley et al., 2006). These mechanics often act in concert with preprogrammed, feed-forward motor commands (such as those from central pattern generators) to generate corrective forces to external perturbations more rapidly than negative feedback alone would allow (Raibert, 1986). Even in the absence of neural feedback, spinalized frogs compensate for phasic perturbations during wiping movements and reach the intended endpoint, and the response is not degraded by deafferentation (Richardson et al., 2005).

When reflex responses are needed to maintain stability, the passive dynamics can simplify the type of neural feedback required. Humans recovering from a trip-up actively control knee flexion while the hip and ankle joints respond according to the passive mechanical interactions with the knee (Eng et al., 1997). By learning the optimum impedance, humans can control arm movements in an unstable environment to achieve stable trajectories where negative feedback alone once failed (Burdet et al., 2001). In such movements, force output is due predominantly to the properties of the mechanical system (Hof, 2003). To be most advantageous, therefore, neural reflexes must be tuned to enhance the stabilizing features of the mechanical system and preflexes, rather than work against them (Hodgins and Raibert, 1991).

The extent to which insects rely on mechanical properties of the musculo-skeletal system to simplify the control of locomotion is largely unknown. Stick insects use neural feedback to stabilize limb trajectories following perturbations in both stance (Bartling and Schmitz, 2000; Cruse et al., 2004)

and swing (Dean, 1984; Dean and Wendler, 1982). Bartling and Schmitz (Bartling and Schmitz, 2000) concluded that while walking at 34 mm s^{-1}, stick insects rely on negative velocity feedback to produce forces opposing lateral or fore–aft substrate perturbations within approximately 75 ms. Stick insects use a different type of control when responding to lateral substrate perturbations depending on substrate stiffness, by relying on efferent copy (Cruse et al., 2004). They produce forces opposing horizontal perturbations during the swing phase in as little as 20 ms, and the compensation during active movements is larger than the resistance reflex of calmly standing animals (Dean, 1984). All of these neural reflexes occur during slow walking. As speed increases, feedback control may suffer due to low reflex gains and long delays in both conduction and force production (Klavins et al., 2002; Rack, 1981).

Cockroaches rely on reflexes to respond to perturbations in ground position or load when standing and walking (Quimby et al., 2006; Ridgel et al., 2001; Zill et al., 2004), and are less effective at climbing inclines and crossing obstacles when subjected to bilateral circumoesophageal connective lesions (Ritzmann et al., 2005). As running speed increases, however, cockroaches appear to rely less on neural reflexes and more on mechanical feedback. For example, cockroaches and spiders maintain high running speeds when crossing a substrate with 90% of the ground surface removed by using distributed mechanical feedback (Spagna et al., 2007). While lizards decrease speed, change kinematics, and insert frequent pauses when crossing obstacles (Kohlsdorf and Biewener, 2006), cockroaches exhibit only minor changes in speed, kinematics or muscle activation patterns while running over unstructured terrain (Sponberg et al., 2004). They rapidly recover from large lateral perturbations to their center of mass (Jindrich and Full, 2002), and their dynamics have been modeled as passive, dynamically self-stabilizing in the face of perturbations (Kubow and Full, 1999). Since both the neural control of slow cockroach locomotion (Delcomyn, 1977; Graham, 1985; Wilson, 1966) and their mechanics during high-speed running (Full et al., 1991; Full and Tu, 1990; Ting et al., 1994) have been well studied, cockroaches are an excellent model for understanding how the nervous system and mechanical properties combine to control rapid running.

The purpose of this study is to determine the role that passive mechanical properties of the leg may play in controlling and stabilizing the rapid running of the cockroach, *Blaberus discoidalis*. The passive hind leg of *Blaberus* is highly damped when subjected to dynamic oscillations (Dudek and Full, 2006). The stiffness and damping parameters from fitting the hysteretic damping model to dynamically oscillated legs predict a rapid recovery from an impulse perturbation. The hysteretic damping model is a simple, linear, two-parameter damped spring (Nashif et al., 1985), used to describe elastomers when material properties are largely independent of strain rate or oscillation frequency. Its two constant parameters accurately predict the cockroach leg response to small amplitude (0.1–1.0 mm) dynamic oscillations over a 240-fold frequency range (0.25–60 Hz). In the present study, we subjected the hind leg to dorso-ventral impulse perturbations to test the hypothesis that the passive exoskeleton can aid recovery during rapid running. Trials on uncontrolled, complex terrain have shown that perturbations from debris are common in the dorso-ventral direction during the swing phase. We examined whether the simple hysteretic damping model could predict the response of the leg to an impulse perturbation. By comparing the animal's response to the model derived to capture dynamic oscillations, we propose the next step toward modeling non-linear, large amplitude impulse perturbations to appendages.

Materials and methods

Animals

Adult, deathhead cockroaches *Blaberus discoidalis* L. of both sexes were obtained from Carolina Biological Supply (Gladstone, OR, USA) and used for all experiments (body mass 3.25±0.25 g, mean ± s.d., N=10). Animals were housed in large plastic containers and fed dried dog food and water *ad libitum.* All cockroaches were euthanized immediately prior to an experiment by placing them in a 237 ml jar saturated with ethyl acetate vapor for 10 min. In dynamic oscillation experiments, the properties of legs from animals euthanized in ethyl acetate did not differ from those from cockroaches euthanized by blocking tracheae with water or from legs amputated from living animals (D.M.D., unpublished data). Experiments were performed at room temperature (24°C).

Impulse perturbations

The response of the left meta-thoracic leg to rapid force perturbations was analyzed to quantify its viscoelastic properties. Dorso-ventrally directed perturbations were applied to the leg in two distinct preparations: one in which the body–coxa joint was free to rotate (free-coxa, Fig. 1A) and the other with the body–coxa joint rigidly fixed (fixed-coxa). Activation of muscles that span the body–coxa joint can stiffen the leg in the dorso-ventral direction, so the two preparations provide bounds to the possible material properties of the leg resulting from muscle activation, with zero activation represented by the free-coxa preparation and maximal activation represented by the fixed-coxa case. Since the joint axes distal to the body–coxa joint are aligned with the perturbation direction (Fig. 1B), muscle activation at these joints should have minimal effect on the leg's viscoelastic response.

To make the experimental set-up as comparable as possible to the dynamic oscillations reported previously (Dudek and Full, 2006), we removed the tarsus and fixed various distal leg joints using cyanoacrylate. While the distal leg joints were not fixed in the dynamic oscillation study, no rotation of these joints was observed in the medio-lateral or antero-posterior directions. In five legs we fixed just the femur–tibia (Fe-Ti) joint because it passively rotates and absorbs energy if left unglued. In another five legs we fixed the coax–trochanter (C-Tr) and trochanter–femur (Tr-Fe) joints in addition. In this manuscript, we will refer to the C-Tr and Tr-Fe joints as a single coxa–trochanter–femur (C-Tr-Fe) joint because the trochanter and femur rotate about the same axis in unison relative to the coxa (Fig. 1B). Furthermore, we mounted the preparations with the body rolled 90° relative to its antero-posterior axis (so that the normally horizontal dorsal plane is

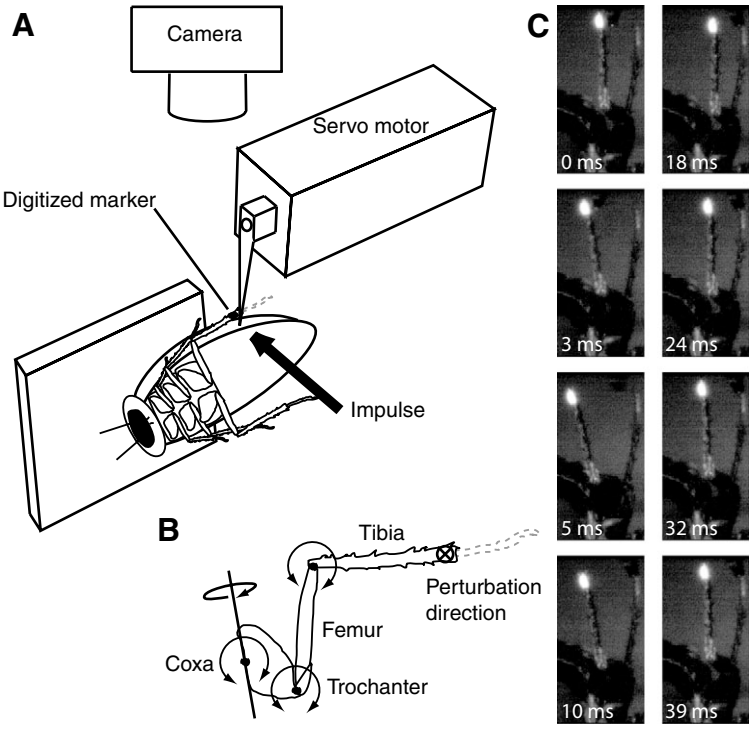

Fig. 1. Experimental setup. (A) In the free-coxa preparation, the dorsal surface of *Blaberus* was attached using epoxy glue to 0.95 cm thick Plexiglas^{TM} and the tarsus removed (broken outline). A servo-motor applied a dorsally directed impulse to the tibia, 1 mm from the distal tip. The free response of the leg was recorded at 1000 frames s^{-1} and the position of a marker 1 mm from the distal tip of the tibia was digitized. The abdomen was pulled dorsally slightly and held so that it did not interfere with the free response of the leg. The fixed-coxa preparation was identical except the leg was removed from the body and glued to the Plexiglas^{TM} at the coxa. In all instances the femur–tibia joint was rigidly fixed by cyanoacrylate, and in half the trials the C-Tr-Fe joint was also rigidly fixed. (B) The joint axes of rotation of the distal joints are parallel with the applied impulse direction (into the page). The body coxa joint's primary axis of rotation runs medio-laterally, so it is free to rotate as a result of the dorsally directed impulse perturbation. The body–coxa joint also has secondary joint axes parallel to the applied impulse. (C) Video frames show the time sequence of the left metathoracic leg's response to an impulse perturbation. The animals's dorsal surface is towards the left of the image while anterior is towards the bottom of the image.

now vertical) to remove the effect of gravity from the leg response (Fig. 1A,C).

In the free-coxa preparation, the thorax was rigidly glued (5 min epoxy) to 0.95 cm thick Plexiglas^{TM}. The abdomen was loosely pulled dorsally so that the leg's recovery from a perturbation was not affected by striking the ventral surface of the abdomen. After perturbing legs with a freely rotating body coxa joint, the legs were removed at the base of the body–coxa joint. The coxa was then rigidly glued to 0.95 cm thick Plexiglas^{TM} (fixed-coxa preparation) in the same orientation as was done in the free-coxa preparation.

We generated perturbations using a lever arm attached to a servo-motor (300B-LR; Aurora Scientific, Aurora, ON, Canada) commanding square waves of 4 ms durations with peak forces of 25, 50 or 75 mN (approximately 1, 2 and 3 times body mass, respectively). The lever arm started in contact with the tibia, 1 mm from the distal end, where a marker (white enamel paint) was placed (Fig. 1A), so that the leg's position and recovery could be recorded at 1000 frames s^{-1} (MotionScopePCI; Redlake, Tucson, AZ, USA).

Controls

There was an approximately 15 min delay between euthanasia and the beginning of tests on the free-coxa preparation. Three impulses were applied to the leg at each of the three peak commanded forces in random order. Tests on the fixed-coxa preparation began within 45 min *post-mortem*, where three impulses each were applied again in random order at the three peak commanded forces. The three position traces at each force level were nearly indistinguishable from one another in both coxa preparations, indicating that material properties were not changing over these short timescales. The traces remained indistinguishable for at least 3 h. As a control, one leg not included in this data set was tested in the fixed-coxa preparation without first undergoing free-coxa perturbations. Its response was not significantly different (P>0.05) from the responses of the other fixed-coxa preparations.

We did not observe *post-mortem* reflex activity or internal hemolymph pressure to affect hind leg properties in a previous study on *Blaberus* (Dudek and Full, 2006), so we did not consider them here. Moreover, we found no effect on leg properties when stimulating either muscle 177c, 177d, 179, 182c, 185 or 194a during a dynamic oscillation. Similarly, living cockroaches wedging against the lever arm of the servo motor in the posterior direction did not have significantly different leg properties compared to euthanized animals when dorso-ventral oscillations were applied.

Data acquisition and parameter calculations

Impulse magnitude

Displacement and force signals from the servo-motor were digitized (board AT-MIO-16E-1; National Instruments, Austin, TX, USA) at 5 kHz and stored to the hard disk of a personal computer (Berta; Transduction Ltd, Mississauga, ON, Canada) running analysis software (Matlab; The Mathworks, Natick, MA, USA). The magnitude of the impulse imparted to the leg (I) was determined by integrating the area under the force signal corresponding to when the lever arm started moving and was in contact with the leg.

Leg position and recovery

The position of the distal end of the tibia was digitized and tracked using commercial software (Motus, Peak Performance). To determine the rate of recovery from the perturbation, we normalized position data in each trial by dividing by the

maximum displacement. The time and percent of perturbation absorbed was then recorded for each peak of the damped free response, as well as the time at which 95% and 99% of the perturbation had been damped.

Modeling leg properties

We calculated the leg's stiffness (k) and structural damping factor (γ) by fitting the recovery trace to the hysteretic damping model (Dudek and Full, 2006; Nashif et al., 1985). The hysteretic damping model gets its name from the fact that it was designed to fit materials whose hysteresis is independent of velocity, and is governed by the equation:

$$F = m\ddot{x} + (1+i\gamma)kx\,, \tag{1}$$

where F is force, m is mass, $\ddot{x}$ is acceleration, x is the position of the leg, and i represents the imaginary number ($\sqrt{-1}$). The response of the model to an idealized unit impulse function in the time domain is:

$$h(t) = \frac{1}{\pi m}\int_0^{\infty}\left(\frac{e^{i\omega t}}{k(1+i\gamma)/m - \omega^2}\right)d\omega\,, \tag{2}$$

where t is time and ω is frequency. Eqn 2 does not have a closed form solution, but can be estimated by numerical integration of:

$$h(t) = \frac{1}{\pi}\int_0^{\infty}\left(\frac{(k-m\omega^2)\cos\omega t + k\gamma\sin\omega t}{(k-m\omega^2)^2 + k^2\gamma^2}\right)d\omega\,. \tag{3}$$

The position of the leg $x(t)$ can be determined for impulses of non-unit magnitude by multiplying $h(t)$ by the impulse magnitude, I.

Stiffness and damping coefficients of the leg were determined by searching for the I, k and γ that minimized the sum of the squared difference between $x(t)$ and the position data from the digitized video. Each leg underwent three impulse perturbations at each commanded force, which were averaged to produce the actual position response. The initial guess for I was therefore the mean measured impulse imparted for each of the three perturbations. The initial guess for k was determined by assuming the frequency of the free response was proportional to $\sqrt{k/m}$, while the initial guess for γ was 0.28 for the free-coxa and 0.2 for the fixed-coxa case [the average damping coefficients determined by dynamic oscillation tests (Dudek and Full, 2006)]. Mass of the free-coxa legs averaged 0.097±0.020 g and the fixed-coxa legs averaged 0.041±0.008 g. The integration range was $0–10^5$ Hz, as recommended by Jones (Jones, 1986).

The impulse response of the hysteretic damping model has been a source of controversy since it is non-causal [$h(t)\neq 0$ for $t<0$] (Crandall, 1963; Milne, 1985). The non-causality arises due to the assumption that k and γ are constants, independent of frequency. If k and γ are allowed to vary with frequency, as they must for all materials over a sufficiently large frequency range, the non-causality disappears (Nashif et al., 1985). For constant parameters, the error in predicted displacement due to the non-causality is very small when $\gamma<0.1$. The error grows as γ increases, and we predict errors of less than 1% for the fixed-coxa and less than 7% for the free-coxa preparations [following Milne (Milne, 1985)].

Statistics

In each preparation, only the left metathoracic limb from each animal was tested. Three-way ANOVAs were performed to examine the relationship of the mechanical properties to coxa preparation, status of the C-Tr-Fe joint, and the impulse magnitude. All tests were performed using statistics software packages (JMP; SAS Institute, Cary, NC, USA; Statistics toolbox; The Mathworks). Unless otherwise stated, all reported values are means ± standard deviations (s.d.).

Results

Applied impulses

A servo-motor was commanded to apply a square-wave force pulse with force amplitudes of 25, 50 and 75 mN of 4 ms duration. Ideally, these commands resulted in applied impulses of 0.1, 0.2 and 0.3 mN s, respectively. For the free-coxa preparation, applied impulses were 0.13±0.04, 0.19±0.06 and 0.19±0.06 mN s, while for the fixed-coxa preparation the impulses were 0.08±0.01, 0.18±0.04 and 0.24±0.05 mN s (N=10 in all cases). By comparison, the forward momentum of the leg at mid-swing is approximately 0.1 mN s (assuming a preferred stride frequency of 10 Hz with a running speed of 0.25 m s^{-1}).

Impulse response

Video frames from a representative free-coxa trial show the typical response to an impulse (Fig. 1C). Stiffness and damping parameters obtained by fitting the hysteretic damping model to leg data from dynamic oscillations predicts that legs respond to impulse perturbations with damped ringing, absorbing most of the perturbation within four cycles (Fig. 2A, Fig. 3A). In both preparations, the response of the distal tip of the tibia showed damped ringing (Fig. 2B, Fig. 3B), oscillating two to four times before coming to rest within 0.04±0.01 mm (mean ± s.e.m., digitizing resolution of 0.02 mm) of the original position. Since impulse magnitude did not have a significant effect on stiffness and damping parameters (Table 1, Table 2), we pooled all the data for the free- and fixed-coxa preparations to examine the time required for the leg to recover from a perturbation (Fig. 4). In all cases, the fixed-coxa legs recovered faster than those with

Table 1. *Effects of coxa-preparation, state of the coxa–trochanter–femur joint, and peak impulsive force on leg stiffness*

Source	d.f.	F	$P>F$
Coxa (body–coxa joint 'fixed' or 'free')	1	166.9	<0.0001
Trochanter (C-Tr-Fe joint 'fixed' or 'free')	1	10.2	0.0025
Force (peak force of 25, 50 or 75 mN)	2	1.6	0.2202
Coxa × trochanter	1	7.8	0.0075
Coxa × force	2	1.7	0.2030
Trochanter × force	2	0.0	0.9651
Coxa × trochanter × force	2	0.0	0.9580
Error	45		
Total	56		

C-Tr-Fe, coxa–trochanter–femur.
Three-way ANOVA with constrained (Type III) sums of squares.
F, F-statistic; $P>F$, probability of greater F-statistic by chance.

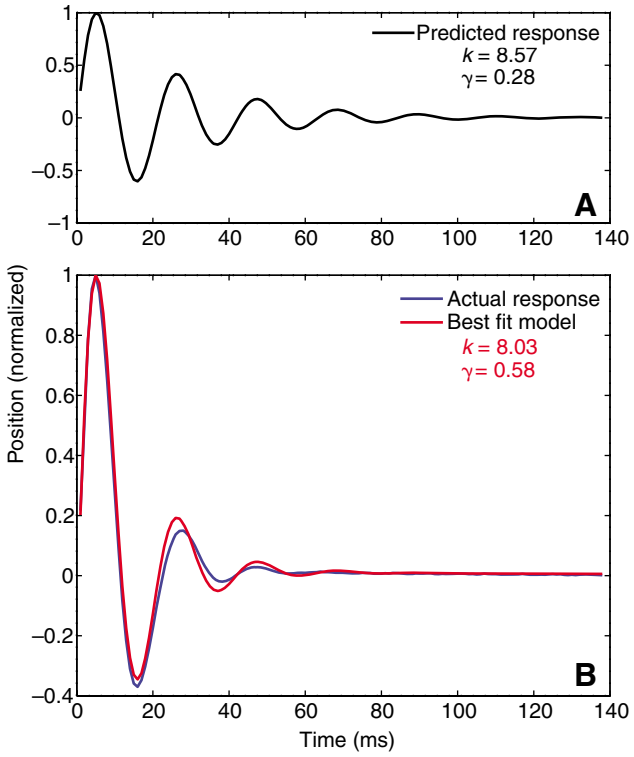

Fig. 2. Response of the metathoracic leg with a freely rotating body–coxa joint to an impulsive perturbation. (A) The predicted free response of a leg based on k and γ from dynamic oscillation experiments (Dudek and Full, 2006). Mass was assumed to be 0.1 g. (B) The actual response of a representative leg with a free body–coxa joint and fixed C-Tr-Fe and femur–tibia joints (blue) compared to the best fit line of the model (red). In all cases, the position is normalized to the peak displacement. The predicted response recovers more than 85% within the time it takes for the actual leg to recover 99%.

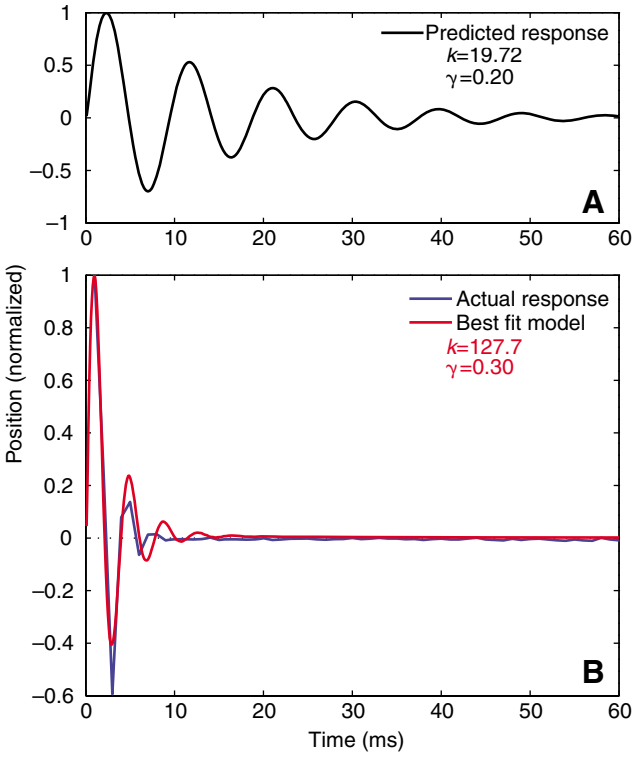

Fig. 3. Response of the metathoracic leg with a fixed body–coxa joint to an impulsive perturbation. (A) The predicted free response of a leg based on k and γ from dynamic oscillation experiments (Dudek and Full, 2006). Mass was assumed to be 0.04 g. (B) The actual response of a representative leg with a fixed body–coxa joint and fixed C-Tr-Fe and femur–tibia joints (blue) compared to the best fit line of the model (red). In all cases, the position is normalized to the peak displacement. The predicted response recovers only 50% within the time it takes for the actual leg to recover 99%.

a freely rotating body–coxa joint (t-test, $P<0.0001$). Legs reached their peak displacement within 4–6 ms, and were 99% recovered within 16±3.3 ms for the fixed-coxa and within 46±6.6 ms for the free-coxa preparations. By comparison, the average swing duration of the hind leg while running at preferred speed is 50–60 ms.

Table 2. *Effects of coxa-preparation, state of the coxa–trochanter–femur joint, and peak impulsive force on leg damping*

Source	d.f.	F	$P>F$
Coxa (body–coxa joint ‘fixed’ or ‘free’)	1	30.9	<0.0001
Trochanter (C-Tr-Fe joint ‘fixed’ or ‘free’)	1	4.7	0.0361
Force (peak force of 25, 50 or 75 mN)	2	1.7	0.1867
Coxa × trochanter	1	0.1	0.7723
Coxa × force	2	1.1	0.3567
Trochanter × force	2	0.2	0.8421
Coxa × trochanter × force	2	0.0	0.9690
Error	45		
Total	56		

C-Tr-Fe, coxa–trochanter–femur.
Three-way ANOVA with constrained (Type III) sums of squares.
F, F-statistic; $P>F$, probability of greater F-statistic by chance.

The dorsally directed perturbation resulted primarily in dorsal-ventral leg motion due to rotation about the medial-laterally directed body–coxa joint axis (Fig. 1B). Peak displacement tended to increase as impulse magnitude increased (Table 3). In the free-coxa preparation, peak dorsal-ventral leg displacement was unaffected (ANOVA, $F=29.73$, $P<0.0001$) by whether or not the C-Tr-Fe joint was fixed, averaging 3.94±1.02 mm when just the femur–tibia was fixed and 3.92±1.13 mm when the C-Tr-Fe was also fixed. Peak average displacement declined in the fixed-coxa preparation, averaging 2.23±0.89 mm with the femur–tibia fixed and declining to 1.28±0.60 mm with the C-Tr-Fe joint fixed as well. There was also motion off the perturbation axis due to smaller rotations about the dorso-ventrally directed body–coxa and coxa–trochanter joint axes (Fig. 1B). While the exact amount of this displacement could not be quantified, it was clear from the videos that fixing the C-Tr-Fe joint led to an increase in off-axis motions.

Viscoelastic model (hysteretic damping)

Impulse response trajectories recreated using the stiffness and damping parameters resulting from fitting a damped

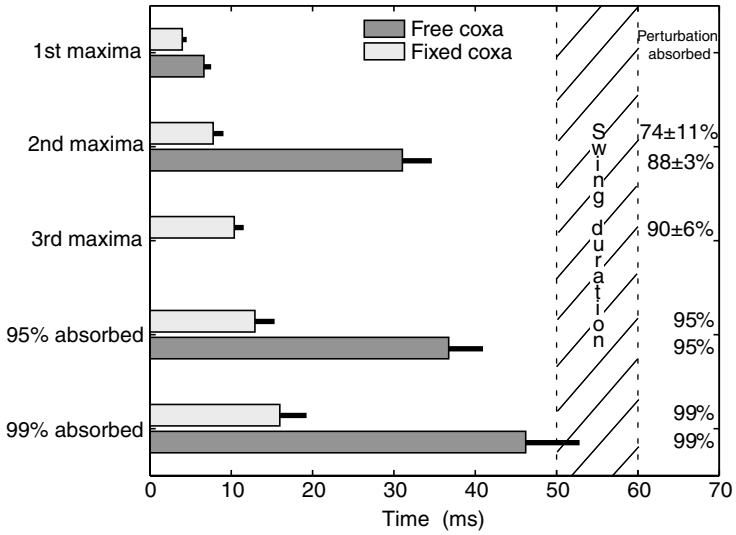

Fig. 4. Free response recovery times. The time it takes to reach individual displacement maxima in the damped response for both the free- (dark grey) and fixed-coxa (light gray) preparations. Bars represent the mean times ± s.d. (N=10). The average swing duration for *B. discoidalis* running at its preferred speed is 50–60 ms. The free-coxa preparation recovers 88% of the perturbation by the second maxima and never has a third maxima with less than 95% absorption. The fixed coxa recovers 74% of the perturbation by the second maxima, 90% by the third, and never has a fourth with less than 95% absorption. In all cases the time to each point is less for the fixed-coxa legs (t-test, P<0.0001) and the time to reach 99% absorption is less than the duration of the swing phase (z-test, P<0.0001).

spring (Eqn 3) to the data closely matched the actual data (Fig. 2B, Fig. 3B). The stiffness and damping parameters depended on whether the body–coxa joint was fixed or free to rotate; they also depended on whether C-Tr-Fe joint was fixed in addition to the femur–tibia (Tables 1, 2). Legs with a fixed coxa were significantly stiffer and less damped (Table 3) than those with a freely rotating coxa (three-way ANOVA, Tukey–Kramer).

Stiffness (k)

Leg stiffness depended on whether the body–coxa joint was fixed or free to rotate, on whether the C-Tr-Fe joint was fixed or free to rotate, and on the interaction between these two parameters (Tables 1, 2). Stiffness was consistently and significantly higher as more joints were fixed, increasing by a factor of 17 between the free- and fixed-coxa preparations and getting 1.5 times stiffer when both the C-Tr-Fe and femur–tibia joints were fixed compared to just fixing the femur–tibia joint (Table 3) alone. Stiffness was independent of the applied impulse magnitude (Tables 1, 3).

Structural damping factor (γ)

The damping factor also depended on both the coxa preparation and how many distal leg joints were fixed, with no interaction between the three grouping variables (Table 2). Fixing the body–coxa joint nearly halved the damping factor while fixing the C-Tr-Fe joint in addition to the femur–tibia led to a small increase in damping (Table 3). Damping factor was independent of the applied impulse magnitude (Tables 2, 3).

Discussion

The passive metathoracic leg of the cockroach recovers from impulsive force perturbations in less time than a single stance or swing phase of a preferred speed stride. Such rapid energy dissipation leads us to suggest that recovering from perturbations during rapid running may be dominated by

Table 3. *Hysteretic damping model parameters*

Coxa preparation	Distal joints fixed	Peak force of impulse (mN)	Peak leg displacement (mm)	k (N m^{-1})	γ
Free	Just femur–tibia	25	2.7±0.2	4.9±0.5	0.80±0.04
		50	4.4±0.4	4.6±0.4	0.67±0.05
		75	4.8±0.6	4.7±0.5	0.63±0.05
	Femur–tibia and C-Tr-Fe	25	2.6±0.4	8.6±0.9	0.95±0.10
		50	4.4±0.6	7.8±0.8	0.80±0.11
		75	4.8±0.8	7.7±1.0	0.74±0.09
Fixed	Just femur–tibia	25	1.2±0.2	74.7±15.0	0.43±0.06
		50	2.3±0.4	109.1±26.9	0.39±0.06
		75	3.2±0.5	80.0±18.1	0.48±0.06
	Femur–tibia and C-Tr-Fe	25	0.7±0.2	120.0±14.8	0.58±0.09
		50	1.3±0.3	156.0±23.0	0.49±0.14
		75	1.9±0.4	135.8±20.2	0.52±0.14

C-Tr-Fe, coxa–trochanter–femur; k, stiffness; γ, structural damping factor.
Values are means ± s.e.m.; N=5 for all cases.

passive mechanical properties of the exoskeleton, thereby simplifying the neural control required for stability. Minimally, no neural control model can ignore the passive mechanical effects of the legs. Stiffness and damping factors determined by applying the one-dimensional hysteretic damping model to dynamic oscillations of the leg (Dudek and Full, 2006) accurately predict that recovery from an impulse perturbation is greater than 90% complete within a single stance or swing phase. This simple, linear model reveals the importance of non-linear leg stiffness and off-axis joint motions in aiding leg recovery. Future efforts to improve our ability to predict the effect of passive mechanical properties on the control of locomotion should include a three-dimensional damping model with a non-linear stiffness component.

Passive leg recovery

The extent to which an insect leg's recovery from a perturbation is mediated by active neural feedback and passive muscle and skeletal properties is likely to depend on speed, with neural feedback playing a larger role during slow movements and self-stabilization arising from passive dynamics playing a larger role as speed increases (Full and Koditschek, 1999). Stick insects walking at one-tenth the preferred speed of *B. discoidalis* appear to rely on negative velocity feedback to control foot position when perturbed during stance, with delays between perturbation onset and rise in leg force of approximately 75 ms (Bartling and Schmitz, 2000). This is more than adequate when stance lasts 1000 ms, but would not suffice when stance only lasts 50 ms. While the short delay of 6–15 ms between transient substrate perturbations of 1–8 mm and tibial campaniform sensilla firing in the cockroach, *P. americana*, is impressively fast (Ridgel et al., 2001), stance lasts only 20–25 ms at their preferred running frequency (Full and Tu, 1991). Since feedback has such a short time window to respond, the passive dynamics could completely determine system behavior at such high running speeds.

During normal running, *B. discoidalis* lifts the distal end of the metathoracic tibia approximately 2.5 mm above the substrate (primarily due to rotation of the body–coxa joint) during each 50–60 ms swing phase. Passive recovery from large perturbations of the leg is rapid, with peak amplitudes reached in 4–6 ms and 99% recovery in less than 50 ms for the most compliant leg orientation, requiring less than 15 ms for the stiffest (z-test, z=–3.14 free body–coxa, z=–56.56 fixed body–coxa, Fig. 4). Such rapid responses may make feedback control of perturbations undesirable during rapid running.

The 6–15 ms latency observed by Ridgel et al. (Ridgel et al., 2001) is consistent with the 10 ms latency observed by Wilson (Wilson, 1965). Adding to this reflex latency is the time required for a muscle to generate force following stimulation, which is 10 ms in *Blaberus* leg muscles (Full and Meijer, 2001). Therefore, the fastest reflex response following a leg perturbation is not likely to occur before 16–20 ms have passed. This prediction is supported by Schaefer et al. (Schaefer et al., 1994), who report the latency between tactile leg stimulus and first leg movement in *P. americana* at 17 ms. For the fixed-coxa case, the leg has fully recovered by then (Fig. 3B, Fig. 4). With a freely rotating body–coxa joint, more than 82% of the perturbation has been absorbed within 20 ms (Fig. 2B). Due to the rapid passive response and reflex delays, neural control models that fail to account for the mechanical properties of the legs will be destabilizing, responding to perturbations that no longer exist (or are greatly reduced). Moreover, actively stretched muscles produce immediate resistance to perturbations (Rack, 1981), so the role of the nervous system in rejecting perturbations at higher speeds may be the feedforward control of overall leg impedance. Due to these muscle preflexes, we predict the response of the leg to a similar perturbation while running will approach the rapid response seen in the fixed-coxa case.

Hysteretic damping model

To test the ability of the hysteretic damping model to predict the leg response under different perturbation regimes, we predicted the leg's response to an impulse using the stiffness and damping factors attained from dynamic oscillations (Dudek and Full, 2006) and compared this prediction to the actual leg response. At an amplitude of 0.5 mm and a frequency of 10 Hz, a dynamically oscillated leg has a stiffness of 8.57±0.57 N m^{-1} (mean ± s.e.m., N=13) for the free-coxa preparation and 19.72±1.24 N m^{-1} (mean ± s.e.m., N=10) for the fixed-coxa. The damping factor was 0.28±0.02 for the free-coxa and 0.20±0.02 for the fixed and the leg mass was assumed to be 0.1 g with the coxa and 0.04 g without the coxa. For the most compliant preparation, where the body–coxa joint is free to rotate (Fig. 2A), the damped ringing occurs at the same frequency as the actual response and 88–92% of the perturbation is recovered within the 50–60 ms duration of a stance or swing phase. While the actual leg has fully recovered by this time (Fig. 4), the model continues ringing with very small amplitudes for another 50–60 ms. The stiffness of the free-coxa preparation with the C-Tr-Fe joint fixed (8.03±1.93 N m^{-1}, Table 3) was the only case where the model parameter from the impulse experiments matched the prediction from dynamic oscillation experiments (P=0.2706, z=–1.09). The predicted impulse response for the stiffest preparation, where the body–coxa joint was rigidly fixed (Fig. 3A), does not match the actual response well (Fig. 3B), capturing neither the ringing frequency nor the time to recover. The fixed-coxa preparation was more than 5 times as stiff as expected (Table 3). Both coxa preparations were 2–3 times as damped as expected (P<0.0001).

Only a small portion of the discrepancy between the impulse response data and the model derived from dynamic oscillations can be accounted for by the fact that the leg is closer to a beam attached to a rotational spring than a point mass attached to a linear spring. For the linear spring, we predict the fixed-coxa leg to have a natural frequency 2.4 times greater than the free-coxa leg. Assuming the leg is a beam, we predict the fixed-coxa preparation with its increased stiffness, shorter length, and decreased mass to have a natural frequency 2.6 times greater than the free-coxa preparation. While the free-coxa leg oscillates very near to the predicted 46 Hz natural frequency, the fixed-coxa leg oscillates at 2–3 times its predicted resonant frequency of 112 Hz.

While we did not expect a precise matching of the model parameters between the two perturbation types, we did expect to be able to predict how stiffness and damping would be affected by the experimental manipulations. Leg stiffness

should increase as fewer joints are free to rotate because joint cuticle is much more compliant than the cuticle of the leg segments (Vincent, 1980). This prediction is supported by our data, where a leg with a rigid body–coxa joint is almost 20 times stiffer than a leg with a freely rotating body–coxa joint and legs with a fixed C-Tr-Fe joint are 50% stiffer than legs with a free C-Tr-Fe joint (Tables 1, 3). Conversely, the structural damping factor should decrease as more joints are immobilized, because leg segments are more resilient than leg joints (Blickhan, 1986; Dudek and Full, 2006; Katz and Gosline, 1992). This prediction is upheld when the body–coxa joint is immobilized and damping is 60% greater for a leg with a freely rotating body–coxa joint (Tables 2, 3). Despite a lower damping factor, a leg with a fixed body–coxa joint recovers faster than one with the joint freely rotating because, while it loses less energy per oscillation, it oscillates at a much higher frequency and losses energy at a higher rate. Interestingly, damping increases 20% when the C-Tr-Fe joint is fixed (Tables 2, 3). This excess damping likely arises due to greater off-axis displacements seen in legs with a rigid C-Tr-Fe joint.

Suggested next steps in modeling

Applying the simplest, linear model to the impulse response of the cockroach leg reveals the importance of non-linear material properties and motions off the perturbation axis in aiding recovery. The leg undergoes deflections following an impulse as much as four times greater than the deflection amplitude of dynamic oscillations. Dynamic oscillations at an amplitude of 1 mm predict a leg stiffness of approximately 20 N m^{-1} (Dudek and Full, 2006), but the slope of the loading curve from 0.7–1.0 mm indicates a stiffness of 35 N m^{-1} over this range. Leg stiffness should continue to increase as displacements approach the 2–4 mm amplitudes produced by impulse perturbations. A linear model cannot take the non-linear leg stiffness of these large deflections into account. Additionally, a one-dimensional model cannot account for energy absorption due to off-axis rotations. Off-axis rotations did not occur during dynamic oscillations because the leg was attached to the lever arm. Here, the leg was free to move in any dimension and off-axis motions could not be prevented. This is because the leg segments are dynamically coupled, so perturbations in one dimension create perturbations to other dimensions (Jindrich and Full, 2002; Kubow and Full, 1999). In this case, the coupling benefits the passive response to a single-axis impulse perturbation by allowing energy absorption to occur simultaneously about multiple axes. To improve biological relevance and predictive power for a leg's response to multiple perturbation types, a three-dimensional, frequency-independent model with non-linear stiffness is required.

Such a model would reduce or eliminate the effects of non-causality. While the hysteretic damping model has analytical solutions for predicting the response to dynamic oscillations, the impulse response must be solved by numerical integration of Eqn 3 across a broad frequency range (0–10^5 Hz). While many biological materials have nearly constant properties across the range of biologically relevant frequencies (Dudek and Full, 2006; Fung, 1984), no material has constant parameters across five frequency decades (Vincent, 1990). This can be a drawback when applying the model when the material has not been characterized across a full frequency spectrum. Using constant parameters to predict the impulse response results in errors in predicted position, particularly as damping factor exceeds 0.1 (Milne, 1985). The damping factors observed in this study (Table 3) yield predicted position errors of 22% for the free-coxa preparation and 10% for the fixed-coxa case. While off-axis motions of the leg occur due to dynamic coupling of the segments, the single degree of freedom model applied here lumps all energy absorption into a single damping factor. A three-dimensional model would allow the damping to be accounted for by three dampers, each with a lower damping factor than that of the one-dimensional model, reducing non-causality errors to an acceptable level.

Conclusions

The hysteretic damping model can predict the timing of response to an impulse perturbation so long as the amplitudes remain low and the leg is compliant. To improve the biological relevance of the model and increase its predictive ability to include larger perturbations and stiffer legs, a three-dimensional model that accounts for off-axis energy absorption and includes a non-linear stiffness term is needed. Due to high stiffness and damping of energy in multiple dimensions, the passive metathoracic leg of the cockroach recovers to within 0.04 mm of its original position following impulsive perturbations of more than twice the leg's peak momentum during a stride in less time than a single stance or swing phase. Such rapid energy dissipation leads us to suggest that recovering from perturbations during rapid running may be dominated by passive mechanical properties of the exoskeleton, thereby simplifying the neural control required for stability.

We thank Dan Goldman and Benson Tongue for helpful discussions on the impulse response of the hysteretic damping model. We thank Tom Libby, Mimi Koehl, Homayoon Kazerooni and two anonymous reviewers for their helpful comments on previous versions of the manuscript. This work was supported by DARPA/ONR – N00014-98-1-0747, DARPA/SPAWAR N66001-03-C-8045 and NSF EF 0425878 FIBR to R.J.F. and a Department of Integrative Biology summer research grant to D.M.D.

References

Bartling, C. and Schmitz, J. (2000). Reaction to disturbances of a walking leg during stance. *J. Exp. Biol.* **203**, 1211.

Blickhan, R. (1986). Stiffness of an arthropod leg joint. *J. Biomech.* **19**, 375-384.

Brown, I. E. and Loeb, G. E. (2000). A reductionist approach to creating and using neuromusculoskeletal models. In *Biomechanics and Neural Control of Posture and Movement* (ed. J. A. Winters and P. E. Crago), pp. 148-163. New York: Springer.

Burdet, E., Osu, R., Franklin, D. W., Milner, T. E. and Kawato, M. (2001). The central nervous system stabilizes unstable dynamics by learning optimal impedance. *Nature* **414**, 446.

Crandall, S. H. (1963). Dynamic response of systems with structural damping. In *Air, Space, and Instruments, Draaper Anniversary Volume* (ed. S. Lees), pp. 183-193. New York: McGraw-Hill.

Cruse, H. (1990). What mechanisms coordinate leg movement in walking arthropods? *Trends Neurosci.* **13**, 15-21.

Cruse, H., Kuhn, S., Park, S. and Schmitz, J. (2004). Adaptive control for insect leg position: controller properties depend on substrate compliance. *J. Comp. Physiol. A* **190**, 983.

Daley, M. A., Usherwood, J. R., Felix, G. and Biewener, A. A. (2006).

Running over rough terrain: guinea fowl maintain dynamic stability despite a large unexpected change in substrate height. *J. Exp. Biol.* **209**, 171.

Daley, M. A., Felix, G. and Biewener, A. A. (2007). Running stability is enhanced by a proximo-distal gradient in joint neuromechanical control. *J. Exp. Biol.* **210**, 383-394.

Dean, J. (1984). Control of leg protraction in the stick insect – a targeted movement showing compensation for externally applied forces. *J. Comp. Physiol.* **155**, 771.

Dean, J. and Wendler, G. (1982). Stick insects walking on a wheel – perturbations induced by obstruction of leg protraction. *J. Comp. Physiol.* **148**, 195.

Delcomyn, F. (1977). Co-ordination of invertebrate locomotion. In *Mechanics and Energetics of Animal Locomotion* (ed. R. M. Alexander and G. Goldspink), pp. 82-114. London: Chapman & Hall.

Dudek, D. M. and Full, R. J. (2006). Passive mechanical properties of legs from running insects. *J. Exp. Biol.* **209**, 1502-1515.

Eng, J. J., Winter, D. A. and Patla, A. E. (1997). Intralimb dynamics simplify reactive control strategies during locomotion. *J. Biomech.* **30**, 581.

Full, R. J. and Koditschek, D. E. (1999). Templates and anchors: neuromechanical hypotheses of legged locomotion on land. *J. Exp. Biol.* **202**, 3325-3332.

Full, R. J. and Meijer, K. (2001). Metrics of natural muscle function. In *Electro Active Polymers (EAP) as Artificial Muscles, Reality, Potential, and Challenges* (ed. Y. Bar-Cohen), pp. 67-83. New York: SPIE and William Andrew/Noyes Publications.

Full, R. J. and Tu, M. S. (1990). Mechanics of six-legged runners. *J. Exp. Biol.* **148**, 129-146.

Full, R. J. and Tu, M. S. (1991). Mechanics of a rapid running insect: two-,four- and six-legged locomotion. *J. Exp. Biol.* **156**, 215-232.

Full, R. J., Blickhan, R. and Ting, L. H. (1991). Leg design in hexapedal runners. *J. Exp. Biol.* **158**, 369-390.

Fung, Y. C. (1984). Structure and stress-strain relationship of soft tissues. *Am. Zool.* **24**, 13-22.

Ghigliazza, R. M., Altendorfer, R., Holmes, P. and Koditschek, D. (2005). A simply stabilized running model. *Siam Rev.* **47**, 519-549.

Graham, D. (1985). Pattern and control of walking in insects. *Adv. Insect Physiol.* **18**, 31-140.

Hodgins, J. K. and Raibert, M. H. (1991). Adjusting step length for rough terrain locomotion. *IEEE Trans. Rob. Autom.* **7**, 289.

Hof, A. L. (2003). Muscle mechanics and neuromuscular control. *J. Biomech.* **36**, 1031-1038.

Holmes, P., Full, R. J., Koditschek, D. and Guckenheimer, J. (2006). The dynamics of legged locomotion: models, analyses, and challenges. *Siam Rev.* **48**, 207-304.

Jindrich, D. L. and Full, R. J. (2002). Dynamic stabilization of rapid hexapedal locomotion. *J. Exp. Biol.* **205**, 2803-2823.

Jones, D. I. G. (1986). The impulse response function of a damped single degree of freedom system. *J. Sound Vibration* **106**, 353-356.

Katz, S. L. and Gosline, J. M. (1992). Ontogenic scaling and mechanical-behavior of the tibiae of the African desert locust (*Schistocerca-Gregaria*). *J. Exp. Biol.* **168**, 125-150.

Klavins, E., Komsuoglu, H., Full, R. J. and Koditschek, D. E. (2002). The role of reflexes versus central pattern generators in dynamical legged locomotion. In *Neurotechnology for Biomimetic Robots* (ed. J. Ayers, J. L. Davis and A. Rudolph). Cambridge, MA: MIT Press.

Kohlsdorf, T. and Biewener, A. A. (2006). Negotiating obstacles: running kinematics of the lizard *Sceloporus malachiticus*. *J. Zool.* **270**, 359-371.

Kubow, T. M. and Full, R. J. (1999). The role of the mechanical system in control: a hypothesis of self-stabilization in hexapedal runners. *Philos. Trans. R. Soc. Lond. B Biol. Sci.* **354**, 849-861.

Milne, H. K. (1985). The impulse-response function of a single degree of freedom system with hysteretic damping. *J. Sound Vibration* **100**, 590-593.

Moritz, C. T. and Farley, C. T. (2004). Passive dynamics change leg mechanics for an unexpected surface during human hopping. *J. Appl. Physiol.* **97**, 1313-1322.

Nashif, A., Jones, D. and Henderson, J. (1985). *Vibration Damping*. New York: John Wiley & Sons.

Quimby, L. A., Amer, A. S. and Zill, S. N. (2006). Common motor mechanisms support body load in serially homologous legs of cockroaches in posture and walking. *J. Comp. Physiol. A* **192**, 247-266.

Rack, P. M. H. (1981). Limitations of somatosensory feedback in control of posture and movement. In *Handbook of Physiology Section 1, The Nervous System, Motor Control*. Vol. II, Pts 1 and 2 (ed. V. B. Brooks), pp. 229-256. Bethesda: American Physiological Society.

Raibert, M. H. (1986). *Legged Robots that Balance*. Cambridge, MA: MIT Press.

Richardson, A. G., Slotine, J.-J. E., Bizzi, E. and Tresch, M. C. (2005). Intrinsic musculoskeletal properties stabilize wiping movements in the spinalized frog. *J. Neurosci.* **25**, 3181-3191.

Ridgel, A. L., Frazier, S. F. and Zill, S. N. (2001). Dynamic responses of tibial campaniform sensilla studied by substrate displacement in freely moving cockroaches. *J. Comp. Physiol. A* **187**, 405.

Ritzmann, R. E., Pollack, A. J., Archinal, J., Ridgel, A. L. and Quinn, R. D. (2005). Descending control of body attitude in the cockroach *Blaberus discoidalis* and its role in incline climbing. *J. Comp. Physiol. A* **191**, 253-264.

Schaefer, P. L., Kondagunta, V. and Ritzmann, R. E. (1994). Motion analysis of escape movements evoked by tactile stimulation in the cockroach, *Periplaneta americana*. *J. Exp. Biol.* **190**, 287-294.

Spagna, J. C., Goldman, D. I., Lin, P. C., Koditschek, D. E. and Full, R. J. (2007). Distributed mechanical feedback in arthropods and robots simplifies control of rapid running on challenging terrain. *Bioinspiration Biomimetics* **2**, 9-18.

Sponberg, S. N., Chang, C. and Full, R. J. (2004). Sensory independent, feedforward control of locomotion in cockroaches running over rough surfaces. *Integr. Comp. Biol.* **44**, 644.

Ting, L. H., Blickhan, R. and Full, R. J. (1994). Dynamic and static stability in hexapedal runners. *J. Exp. Biol.* **197**, 251-269.

Vincent, J. F. V. (1980). Insect cuticle: a paradigm for natural composites. *Symp. Soc. Exp. Biol.* **34**, 183-210.

Vincent, J. F. V. (1990). *Structural Biomaterials*. Princeton: Princeton University Press.

Wilson, D. M. (1965). Proprioceptive leg reflexes in cockroaches. *J. Exp. Biol.* **43**, 397-409.

Wilson, D. M. (1966). Insect walking. *Annu. Rev. Entomol.* **11**, 103-123.

Zill, S., Schmitz, J. and Buschges, A. (2004). Load sensing and control of posture and locomotion. *Arthropod Struct. Dev.* **33**, 273-286.